environmental microbiology

Environmental Microbiology (2010) **12**(2), 541–556 doi:10.1111/j.1462-2920.2009.02113.x

Microbial functional structure of *Montastraea faveolata*, an important Caribbean reef-building coral, differs between healthy and yellow-band diseased colonies

Nikole E. Kimes,[1,2,3] Joy D. Van Nostrand,[4,5] Ernesto Weil,[6] Jizhong Zhou[4,5] and Pamela J. Morris[1,2,3,7]*

[1]*Marine Biomedicine and Environmental Sciences Center, Medical University of South Carolina, Charleston, SC, USA.*

[2]*Department of Molecular and Cellular Biology and Pathobiology, Medical University of South Carolina, Charleston, SC, USA.*

[3]*Hollings Marine Laboratory, Charleston, SC, USA.*

[4]*Institute for Environmental Genomics and Department of Botany and Microbiology, University of Oklahoma, Norman, OK, USA.*

[5]*Virtual Institute for Microbial Stress and Survival, Lawrence Berkeley, National Laboratory, Berkeley, CA, USA, http://vimss.lbl.gov*

[6]*Department of Marine Sciences, University of Puerto Rico, Mayaguez, Puerto Rico.*

[7]*Department of Biology, College of Charleston, Charleston, SC, USA.*

Summary

A functional gene array (FGA), GeoChip 2.0, was used to assess the biogeochemical cycling potential of microbial communities associated with healthy and Caribbean yellow band diseased (YBD) *Montastraea faveolata*. Over 6700 genes were detected, providing evidence that the coral microbiome contains a diverse community of archaea, bacteria and fungi capable of fulfilling numerous functional niches. These included carbon, nitrogen and sulfur cycling, metal homeostasis and resistance, and xenobiotic contaminant degradation. A significant difference in functional structure was found between healthy and YBD *M. faveolata* colonies and those differences were specific to the physical niche examined. In the surface mucopolysaccharide layer (SML), only two of 31 functional categories investigated, cellulose degradation and nitrification, revealed significant differences, implying a very specific change in microbial functional potential. Coral tissue slurry, on the other hand, revealed significant changes in 10 of the 31 categories, suggesting a more generalized shift in functional potential involving various aspects of nutrient cycling, metal transformations and contaminant degradation. This study is the first broad screening of functional genes in coral-associated microbial communities and provides insights regarding their biogeochemical cycling capacity in healthy and diseased states.

Received 16 July, 2009; accepted 14 October, 2009. *For correspondence. E-mail morrisp@cofc.edu; Tel. (+1) 843 762 8803; Fax (+1) 843 763 8737.

Introduction

Coral ecosystems are being degraded worldwide due in large part to disease outbreaks (Harvell *et al*., 2007; 2009). Caribbean yellow band disease (YBD) affects all four species of the *Montastraea* genus, causing significant tissue and colony mortality in some of the most important Caribbean reef-building corals (Croquer and Weil, 2009; Harvell *et al*., 2009). The prevalence and virulence of YBD has increased over the past decade and poses a significant risk to the stability of some Caribbean coral ecosystems (Bruckner and Bruckner, 2006; Weil *et al*., 2006; Croquer and Weil, 2009; Harvell *et al*., 2009). To better understand the etiology of YBD and other coral diseases, scientists have examined the microbial communities associated with corals (Leggat *et al*., 2007; Rosenberg *et al*., 2007 and references therein). As a result, these communities are increasingly recognized as important components of the coral holobiont that influence coral health and disease (Rosenberg and Loya, 2004; Coral Disease Working Group, 2007; Rosenberg *et al*., 2007).

Endosymbiotic dinoflagellates of the genus *Symbiodinium*, or zooxanthellae, were the first microbial community shown to associate with corals (Yonge, 1929; 1931). They contribute to the health of the coral holobiont through provision of nutrients and oxygen via photosynthesis (Goreau and Goreau, 1960; Goreau *et al*., 1979); disruption of this relationship results in bleaching and coral disease (Cervino *et al*., 2001; 2004; Baker, 2003; Thornhill *et al*., 2006). In addition to the zooxanthellar community, studies reveal distinct bacterial (Rohwer *et al*., 2001; 2002; Bourne and Munn, 2005; Klaus *et al*.,

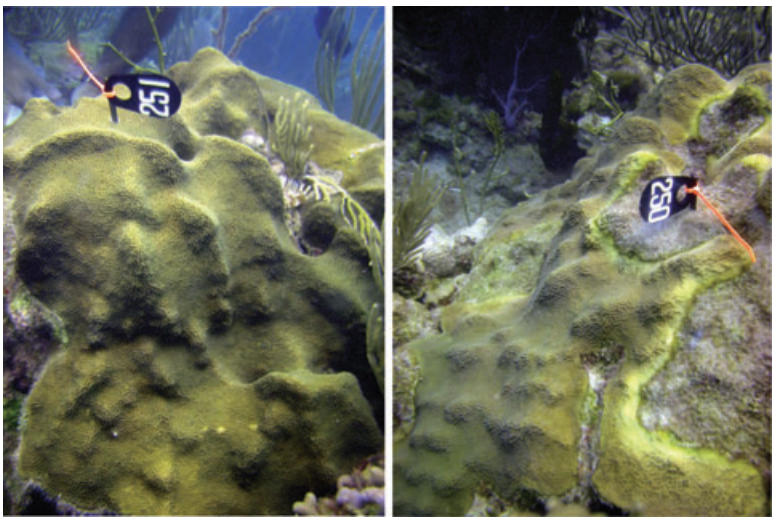

Fig. 1. Digital images of two *M. faveolata* colonies, one healthy (left) and one YBD (right), tagged and sampled in March 2007 from the Media Luna Reef of La Parguera, Puerto Rico. (Photos E. Weil)

2005; Koren and Rosenberg, 2006; Yokouchi *et al.*, 2006; Wegley *et al.*, 2007), archaeal (Kellogg, 2004; Wegley *et al.*, 2004; Siboni *et al.*, 2008) and fungal (Bentis *et al.*, 2000; Wegley *et al.*, 2007) communities associated with reef-building corals. Additional evidence reveals variation in the microbial community structure between healthy and diseased (or stressed) colonies, implicating them in the maintenance of a healthy environment for the coral holobiont (Casas *et al.*, 2004; Sekar *et al.*, 2006; Bourne *et al.*, 2007; Coral Disease Working Group, 2007; Rosenberg *et al.*, 2007; Lampert *et al.*, 2008; Sunagawa *et al.*, 2009; Thurber *et al.*, 2009).

The functional role of the zooxanthellae is well established in the coral holobiont (Yonge, 1931; Muscatine, 1973; 1980; 1990; Goreau *et al.*, 1979; Muscatine *et al.*, 1984; Muller-Parker and D'Elia, 1997; Knowlton and Rohwer, 2003; Stat *et al.*, 2008) and thus will not be discussed here. In contrast, the role of the bacterial, archaeal and fungal communities is not yet fully characterized, although there is speculation regarding their role in nutrient cycling. For example, nitrogen cycling is often cited as a probable role filled by the microbial community (Rohwer *et al.*, 2002; Rosenberg *et al.*, 2007; Wegley *et al.*, 2007). This assumption is supported by indirect evidence including acetylene reduction activity in coral colonies (Shashar *et al.*, 1994), excretion of ammonium from the endolithic community (Szmant *et al.*, 1990; Ferrier-Pages *et al.*, 1998), and the presence of bacteria capable of nitrogen cycling (Frias-Lopez *et al.*, 2002; Rohwer *et al.*, 2002; Lesser *et al.*, 2004; Yokouchi *et al.*, 2006; Wegley *et al.*, 2007; Olson *et al.*, 2009). Even less is known about the functional role of archaea and fungi in the coral holobiont; however, both are implicated in nitrogen cycling as well. The presence of the ammonia monooxygenase gene, amoA, in coral associated crenarchaeota suggests a potential role in nitrification (Beman *et al.*, 2007; Siboni *et al.*, 2008); while metagenomic data provide evidence suggesting a role for fungi in ammonification and ammonia assimilation (Wegley *et al.*, 2007). Additionally, the presence of both sulfate-oxidizing and sulfate-reducing bacteria in the coral holobiont implicates a possible role for the microbial community in sulfur cycling (Richardson, 2004; Barneah *et al.*, 2007; Raina *et al.*, 2009).

Determining the functional role of complex and dynamic microbial communities is challenging due to our inability to culture the vast majority (~99%) of microorganisms (Amann *et al.*, 1995; Fuhrman and Campbell, 1998). To address this challenge, high-throughput functional gene arrays (FGA) are being used to probe for genes involved in specific functions of interest (Wu *et al.*, 2001; Gentry *et al.*, 2006; He *et al.*, 2007). The most comprehensive FGA currently available, the GeoChip 2.0, uses 24 243 oligonucleotide (50-mer) probes to target ~10 000 known microbial biogeochemical cycling genes involved in carbon, nitrogen and sulfur cycling, metal homeostasis and resistance, and xenobiotic contaminant degradation. The functional structure of complex microbiomes from various environments has been examined using the GeoChip 2.0, including contaminated aquifers (Rodriguez-Martinez *et al.*, 2006; Van Nostrand *et al.*, 2009), contaminated ground water (Wu *et al.*, 2006; He *et al.*, 2007; Waldron *et al.*, 2009), tropical marine sediments (Wu *et al.*, 2008), soils (Yergeau *et al.*, 2008), crude oil-contaminated soils (Liang *et al.*, 2009), marine basalts (Mason *et al.*, 2009) and deep sea hydrothermal vents (Wang *et al.*, 2009). These studies indicated that GeoChip is a powerful tool for analysing microbial community functional structure from a variety of habitats.

The aim of this study is to characterize the biogeochemical cycling potential of microbial communities associated with healthy and YBD *M. faveolata* (Fig. 1).

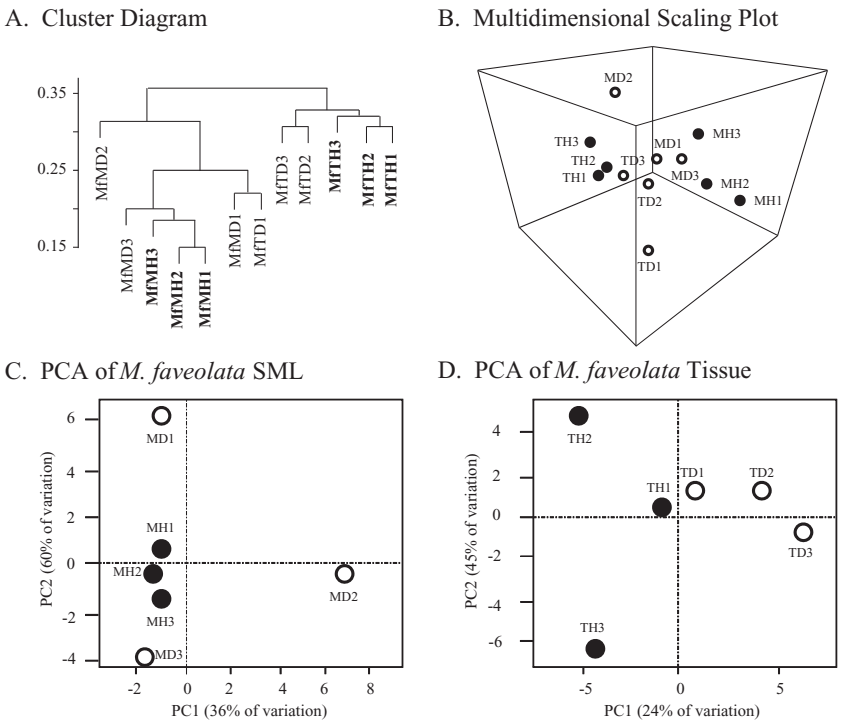

Fig. 2. Multivariate analysis of functional genes associated with *M. faveolata*.
A. Cluster analysis of the functional genes detected in healthy (bolded) and YBD *M. faveolata*. SML (M) and tissue slurry (T).
B. Multidimensional scaling plot of the functional genes detected in healthy (filled circles) and YBD (open circles) *M. faveolata* SML (M) and tissue slurry (T).
C. PCA of the functional genes detected in healthy (filled circles) and CYBD (open circles) *M. faveolata* SML.
D. PCA of the functional genes detected in healthy (filled circles) and CYBD (open circles) *M. faveolata* tissue slurry.

The multitude of bacterial, archaeal and fungal genes detected across all *M. faveolata* samples (biological triplicates of: healthy surface mucopolysaccharide layer (SML), healthy tissue slurry, YBD SML and YBD tissue slurry; $n = 12$), using the GeoChip, is reported. In addition, evidence revealing differences in functional potential between healthy and YBD *M. faveolata* SML and tissue slurry is presented. Based on our findings, the diversity of functional genes detected and their implication in nutrient cycling for the coral holobiont are discussed.

Results

Comparison of the functional structure in M. faveolata *SML and tissue slurry*

Cluster analysis of our data revealed a distinct separation between the *M. faveolata* SML and tissue slurry samples, with the exception of one sample (Fig. 2A). We detected an average of 1213 genes in the SML, whereas, the average number of genes detected in the tissue slurry was 2656, revealing a significant difference in the number of genes detected (*t*-test, $P = 0.004$). Additionally, both the Shannon–Wiener (H′) and Simpson's Reciprocal 1/D diversity indices indicate higher levels of genetic diversity in *M. faveolata* tissue slurry than that seen in the *M. faveolata* SML samples, with both tissue and SML-associated communities exhibiting similar Shannon–Wiener's evenness (Table 1).

Comparison of the functional structure between healthy and YBD M. faveolata

The number of genes detected varied between healthy and YBD samples within both the SML and tissue slurry (Table 1). In the SML, an average of 947 total genes were detected in the healthy samples; whereas, an average of 1484 total genes were detected in the YBD samples. Furthermore, the number of unique genes associated with healthy SML samples (306) was much smaller than the number identified in the YBD SML samples (1365). Tissue samples exhibited the opposite trend with the healthy samples showing a slightly larger average number of detected genes (3037) than that of the YBD tissue samples (2275). The number of unique genes detected in *M. faveolata* healthy tissue samples (1424) was also greater than that detected in the YBD tissue samples (892).

Cluster analysis of the functional genes identified for each sample showed two distinct clusters for healthy *M. faveolata* SML and healthy *M. faveolata* tissue slurry samples, while the YBD SML and tissue slurry samples exhibited more variability in their clustering pattern (Fig. 2A). This trend is also visible using a non-metric multidimensional scaling plot (Fig. 2B). To determine if the functional structures of healthy and YBD *M. faveolata* were significantly different, a two-way crossed analysis of symmetry (ANOSIM), the approximate analogue of a two-way ANOVA, was performed. This analysis accounts for

Table 1. Functional gene diversity of *M. faveolata*-associated microorganisms.

	M. faveolata SML						*M. faveolata* tissue slurry					
	Healthy			YBD			Healthy			YBD		
	H1	H2	H3	D1	D2	D3	H1	H2	H3	D1	D2	D3
Colony ID												
H1	**110**	*496*	*426*	*676*	*508*	*369*	**489**	*1798*	*1509*	*1612*	*1468*	*783*
H2		**104**	*500*	*729*	*472*	*408*		**640**	*1646*	*1723*	*1571*	*850*
H3			**92**	*616*	*408*	*352*			**295**	*1466*	*1335*	*833*
D1				**302**	*699*	*537*				**460**	*1547*	*767*
D2					**734**	*447*					**378**	*740*
D3						**329**						**54**
Total genes detected	970	1010	861	1618	1739	1089	3066	3404	2642	2982	2667	1175
Diversity indices												
Simpson's reciprocal index (1/D)	504	467	383	821	838	553	1593	1620	1417	1458	1415	678
Shannon–Weiner index (H')	6.58	6.56	6.38	7.06	7.16	6.66	7.72	7.79	7.60	7.65	7.59	6.81
Shannon evenness	0.96	0.95	0.94	0.96	0.96	0.95	0.96	0.96	0.96	0.96	0.96	0.96

The genes detected for each *M. faveolata* SML or tissue sample were compared with that of the other SML or tissue samples to determine the number of unique and overlapping genes between each sample pair. The boldface numerical values represent the number of unique genes, while the italicized values represent the number of overlapping genes between two samples. The diversity indices were calculated for each sample using software provided by the Institute for Environmental Genomics at the University of Oklahoma (http://ieg.ou.edu/).

variation in one parameter (SML and tissue slurry) when determining similarity within a second parameter (healthy and YBD). The ANOSIM revealed significant dissimilarity between the microbial functional structure of healthy and YBD *M. faveolata* ($R = 0.42$, $P < 0.01$). The ANOSIM also showed dissimilarity between the SML and tissue slurry; however, it was less significant ($R = 0.46$, $P < 0.07$) than that seen between healthy and YBD.

Changes between healthy and YBD functional structures in the SML and the tissue slurry were also examined separately due to the differences observed between the SML and tissue slurry samples in the cluster analysis and ANOSIM results. Principal component analysis (PCA) shows two distinct trends distinguishing healthy and YBD samples in either the *M. faveolata* SML (Fig. 2C) or tissue slurry (Fig. 2D). The healthy SML samples cluster together; whereas, the YBD SML samples show a great deal of variation between one another and in comparison to the healthy SML. In contrast, the microbial community associated with *M. faveolata* tissue slurry shows clear separation between the healthy and YBD colonies; however, there is also variation among both the healthy and YBD communities.

One-way ANOSIMs were run for each functional category using only the SML samples or the tissue slurry samples. Our findings revealed specific changes in the two different environments, further supporting the distinct trends observed using PCA results. Only two of the 31 functional categories investigated, cellulose degradation and nitrification, revealed significant differences ($P < 0.1$) when looking at coral SML samples, implying a specific change in microbial functional potential (Fig. 3). A significantly larger number of cellulase genes (169) were detected in YBD samples than in healthy samples (97). This represents a 47% increase in the number of genes detected; interestingly, the increase in total signal intensity of cellulase genes was only 18%. Similar to the cellulose degradation category, the number of nitrification genes associated with YBD *M. faveolata* SML (46) was 60% higher than that associated with the healthy SML (28). The healthy-associated nitrification genes were identified as bacterial *amoA* (26) and *hao* (2) genes; while the YBD-associated genes represented 40 *amoA*, four *amoB*, one *amoC* and one *hao* bacterial genes.

In contrast to the SML samples, the tissue slurry samples revealed significant changes ($P < 0.1$) in 10 of the 31 categories examined (carbon fixation, cellulose degradation, lignin degradation, nitrification, copper resistance/reduction, benzene by-product degradation, BTEX degradation, nitroaromatics degradation and pesticide/fungicide/herbicide degradation), suggesting a more generalized shift in functional potential involving various aspects of nutrient cycling, metal transformations and contaminant degradation.

Overview of biogeochemical cycling genes identified

Across all *M. faveolata* samples (biological triplicates of healthy SML, healthy tissue slurry, YBD SML and YBD tissue slurry; $n = 12$), a total of 6727 functional genes were detected, with each sample showing significant hybridization to genes in all 31 functional categories investigated (Table 1). Bacterial, archaeal and fungal genes were represented in 31, 24 and 15 of the categories examined respectively (Table 2). Approximately half of the genes were nutrient cycling genes involved in the

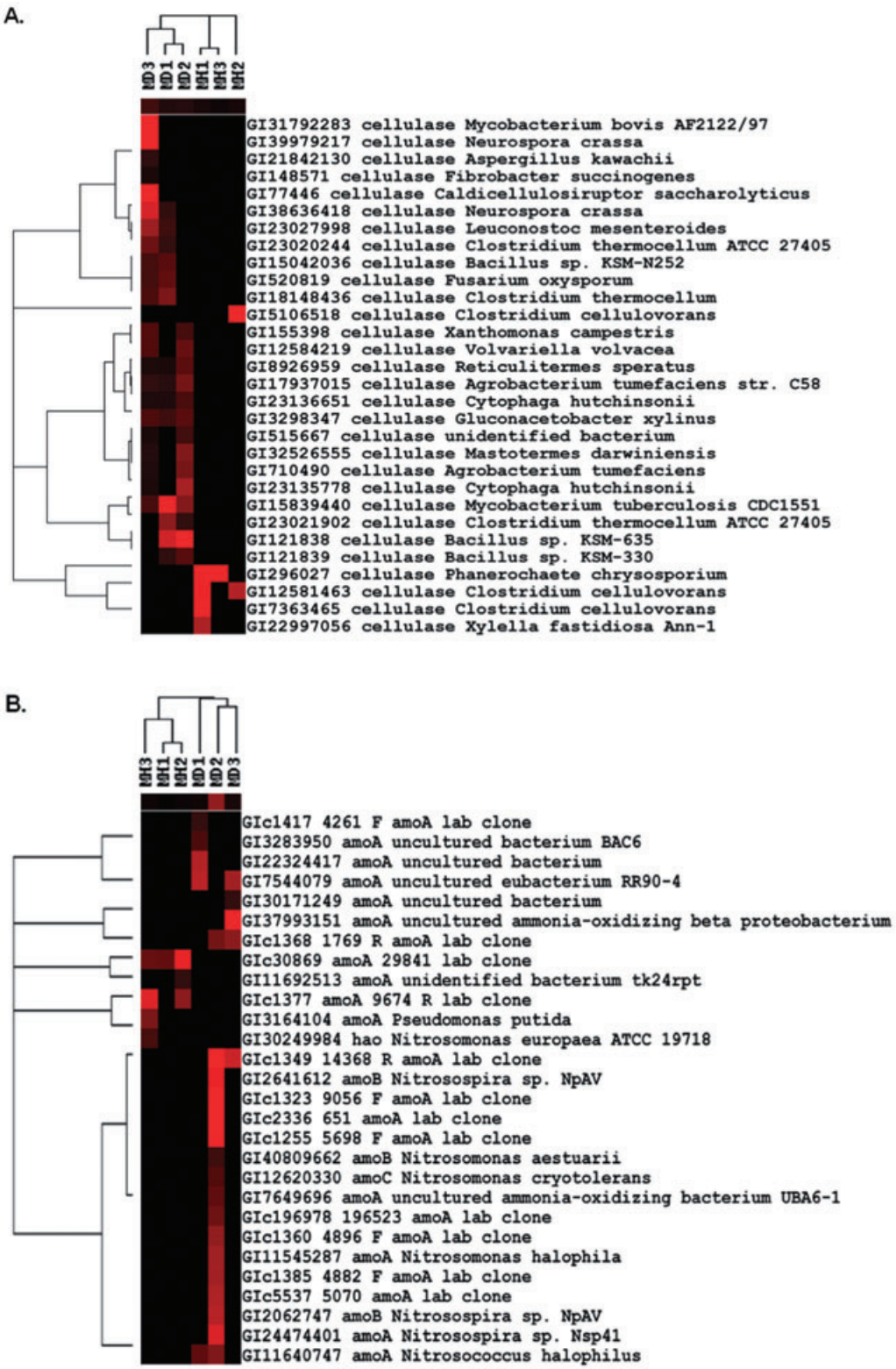

Fig. 3. Heat maps of the signal intensity for a subset of cellulase genes (A) and nitrification genes (B) detected in either healthy only (MH1-3) or YBD only (MD1-3) SML samples.

Table 2. Biogeochemical cycling categories examined and the number of genes detected across all *M. faveolata* samples ($n = 12$) for each category.

Functional category	Number of genes
Carbon cycling	1289
Carbon fixation[A,B]	262
Cellulose degradation[A,B,C]	360
Chitin degradation[A,B,C]	206
Lignin degradation[C]	113
Other polysaccharide degradation[A,B,C]	146
Methane production[A,B]	108
Methane oxidation[B]	111
Nitrogen cycling	1449
Nitrogen fixation[A,B]	311
Nitrification[B]	134
Assimilation/ammonification[A,B,C]	320
Denitrification[A,B,C]	584
Sulfur cycling[A,B]	501
Metal homeostasis and resistance	1309
Arsenic resistance/reduction[A,B,C]	239
Cadmium resistance/reduction[A,B,C]	69
Chromium resistance/reduction[A,B,C]	96
Copper resistance/reduction[A,B,C]	144
Iron uptake[B]	247
Mercury resistance/reduction[A,B]	155
Nickel resistance/reduction[A,B]	43
Tellurium/selenium resistance/reduction[B]	183
Zinc resistance/reduction[A,B,C]	33
Other metal transformations[A,B,C]	100
Xenobiotic contaminant degradation	2162
Benzene by-product degradation[A,B,C]	825
BTEX and related aromatic degradation[A,B]	102
Chlorinated aromatic degradation[B]	53
Chlorinated solvent degradation[B]	40
Heterocyclic aromatic degradation[B]	120
Hydrocarbon (e.g. PAHs) degradation[A,B]	209
Nitroaromatic degradation[A,B,C]	168
Pesticide/fungicide/herbicide degradation[A,B]	138
Other xenobiotic contaminant degradation[A,B,C]	507
Total genes identified	6727

The superscript letters 'A' (archaea), 'B' (bacteria) and 'C' (fungi) indicate the microbial communities identified for each category.

transformation of carbon (19.2%), nitrogen (21.9%) and sulfur (7.5%). The remaining genes detected were involved in metal homeostasis and resistance (19.3%) and xenobiotic contaminant degradation (32.1%). Despite significant differences in the number of genes detected between samples, the relative abundance (i.e. percentage of each category) of functional categories revealed a consistent pattern across all samples (Fig. 4), suggesting functional redundancy in microbial communities.

Carbon cycling genes detected

Carbon dioxide is most often assimilated into organic compounds during photosynthesis through the Calvin cycle, in which ribulose-1,5-bisphosphate carboxylase/oxygenase (*rbcL*) catalyses the carboxylation of ribulose ultimately resulting in the formation of two glyceraldehydes 3-phosphate molecules (Berg *et al.*, 2002; Badger and Bek, 2008). In this study, we detected 134 *rbcL* genes belonging to archaea (5) and bacteria (129). Of the bacterial *rbcL* genes detected, most were identified either as *Proteobacteria* (66), including the subclasses *Alpha-*, *Beta-*, *Delta-* and *Gammaproteobacteria*, or *Cyanobacteria* (27), with the subclasses *Nostocaceae*, *Chroococcales* and *Prochlorophytes* represented. Alternative pathways used in carbon dioxide assimilation include the reductive acetyl-CoA pathway (Ragsdale, 1991) and the reverse Krebs cycle (Buchanan and Arnon, 1990). We detected 9 species of the acetyl-CoA carboxylase (*acc*) gene, which codes for an enzyme involved in the reductive acetyl-CoA pathway, including 5 Crenarachaeota, 2 *Euryarchaeota* and 2 *Clostridium* species. The remaining 119 genes detected were involved in the reverse Krebs cycle and mainly represented uncultured bacteria and *Proteobacteria*.

We detected 825 microbial genes involved in carbon degradation. The majority of genes detected were involved in polysaccharide degradation; these included bacterial, archaeal and fungal cellulases (359 sequences), chitinases (206 sequences), mannanases (55 sequences) and polygalactases (63 sequences). Additionally, 113 sequences for laccase, an enzyme necessary for the decomposition of recalcitrant liginin compounds, were identified as fungal species. The remaining

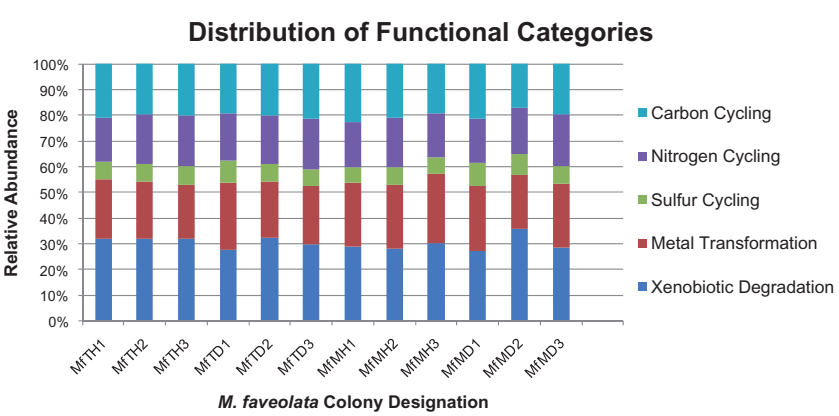

Fig. 4. Comparison of functional variations in the microbiome of *M. faveolata*. Relative abundance (total signal intensity for all genes detected in a given category/total signal intensity) of the five major biogeochemical cycling categories is shown across all 12 *M. faveolata* samples examined. MfTH1-3, biological triplicates of healthy tissue slurry; MfTD1-3, biological triplicates of YBD tissue slurry; MfMH1-3, biological triplicates of SML; MfMD1-3, biological triplicates of YBD SML.

genes detected included 6-phosphogluconolactonase (*pgl*), an enzyme involved in the pentose phosphate pathway.

The present study utilized sequences from two variants of the methane monooxygenase (*mmo/pmo*) gene to characterize aerobic methane oxidation; while sequences for the methyl-coenzyme M reductase (mcr) gene were used to characterize methanogenesis and anaerobic oxidation of methane. We detected 106 *mmo/pmo* genes, representing uncultured putative methanotrophs (58%), type I methanotrophs (25%) and type II methanotrophs (17%). Type I methanotrophs are *Gammaproteobacteria*, whereas, type II are *Alphaproteobacteria* (Hanson and Hanson, 1996). The archaeal *mcr* genes detected (108) were dominated by five groups: *Methanobacteriales*, *Methanococcales*, *Methanomicrobiales*, *Methanosarcinales* and *Methanopyrales*.

Nitrogen cycling genes detected

Nitrogen fixation occurs when diazotrophs convert inert atmospheric nitrogen gas (N_2) into ammonium using the highly conserved nitrogenase enzyme complex (Zehr *et al*., 2003). Nitrogenase (*nifHDK*) contains two principle components, and they are represented on the GeoChip 2.0 by *nifD* (component I) genes and *nifH* (component II) genes. The majority (~70%) of these genes detected, 18 *nifD* and 293 *nifH*, were identified as uncultured or unidentified bacterial species associated with both terrestrial and marine ecosystems. The remaining bacterial genes were from *Proteobacteria* (8%), *Cyanobacteria* (6%), *Firmicutes* (5%) and *Spirochetes* (2%). Additionally, 13 methanogenic *Euryarchaeota* genes were identified.

Ammonia monooxygenase (*amo*) is a microbial enzyme that catalyses the oxidation of ammonia to hyproxylamine, the first step in nitrification; subsequently, the enzyme hydroxylamine oxidoreductase (*hao*) catalyses the reduction of hydroxylamine to nitrite. In our study, 130 *amoABC* genes were detected. The majority (~54%) of *amo* genes were identified as uncharacterized laboratory clones; the remaining 48% were unidentified bacteria (24%), *Betaproteobacteria* (18%) and *Gammaproteobacteria* (6%). Additionally, two *Betaproteobacteria hao* genes were detected.

Denitrification involves the reduction of nitrate to nitrite, nitric oxide, nitrous oxide and finally N_2 (Jetten, 2008). The GeoChip 2.0 contains probes for four different enzymes involved in denitrification, including nitrate reductase (*nar*), nitrite reductase (*nir*), nitric oxide reductase (*nor*) and nitrous oxide reductase (*nos*). Overall, 584 denitrification genes were identified in association with *M. faveolata*. Of the 141 *nar* genes detected, *Proteobacteria* and *Firmicutes* were identified as the predominant (81%) classes represented, while 9% were *Cyanobacterial narB* genes. Multiple subunits of the *nir* gene were also detected, totalling 226 *nirABDKS* genes. Although the majority (63%) of *nir* genes originated from uncultured bacteria, two genes represented *Euryarchaeota* species and two more represented fungal species. All of the 40 *norB* genes detected were of bacterial origin, with 25% representing *Proteobacteria* and 75% representing uncultured bacteria. Similarly, all 85 *nosDZ* genes were of bacterial origin from either *Proteobacteria* (18%) or uncultured bacteria from environmental samples (82%).

Nitrogen cycling can also occur through the metabolism of organic nitrogen sources, such as glutamate and urea. Nitrogen assimilation is the process by which organisms incorporate either nitrites/nitrates or ammonia into organic forms of nitrogen; conversely, biological nitrogen can be reduced to ammonia for recycling through nitrogen mineralization and/or ammonification. The metabolism of glutamate via the enzyme glutamate dehydrogenase (*gdh*) is one example. In this study, we detected 43 *gdh* genes from 14 species of archaea, including both *Crenarchaeota* and *Euryarchaeota*, as well as 29 species of bacteria representing 6 different classes. In addition, we detected 16 *gdh* genes originating from fungi. The degradation of urea via the urease enzyme is another example known to occur in corals (Barnes and Crossland, 1976). We detected 358 microbial urease genes. The vast majority (95%) were identified as bacterial species, mainly from the class *Proteobacteria* with some *Cyanobacteria*, *Firmicutes* and *Actinobacteria* species also identified. In addition, archaeal (*Crenarchaeota* and *Euryarcheota*) and fungal urease genes were identified.

Sulfur cycling genes detected

Using the GeoChip, we detected 501 sequences of the *dsr* gene. Approximately half of the *dsr* genes were identified as uncultured bacteria; the remaining bacterial genes were identified as *Deltaproteobacteria* (22%), *Clostridia* (6%), *Thermosulfobacteria* (1%), *Chlorobia* (1%) and *Nitrosporirae* (1%). Six archaeal species from the *Euryarchaeota* classes of *Archaeolglobi* and *Methanobacteria* were also identified. Although it has previously been suggested that organic sulfur plays a larger role in coral-associated sulfur cycling than that of inorganic sulfur (Wegley *et al*., 2007), the vast number of *dsr* genes identified suggests that the metabolism of inorganic sulfur is important to the health of the coral holobiont.

Metal homeostasis and resistance genes detected

Due to the ubiquitous presence of heavy metals and their potential toxicity, microorganisms have developed various strategies for regulating both trace and major elements (Lloyd, 2005). The GeoChip contains probes for metal

homeostasis and resistance mechanisms, such as transport systems, resistance proteins and efflux mechanisms. Of the 1306 metal-associated genes detected, the most abundant were involved in iron (19%), arsenic (18%), tellurium (13%), mercury (12%) and copper (11%) regulation. Both iron and copper are biologically necessary for all organisms, while arsenic and tellurium may be biologically relevant in some microorganisms; mercury, however, has no known physiological benefits. All of these elements can be toxic at certain concentrations and therefore require strict regulatory mechanisms (Silver and Phung, 2005).

Xenobiotic degradation genes detected

The recalcitrant quality of xenobiotic compounds results from a lack of enzymes required for their degradation and may result in detrimental effects. The enzymes and proteins involved in xenobiotic degradation often facilitate the degradation of synthetic molecules produced through industry; however, they also degrade natural compounds. Both functions are important, and communities that harbour a diverse range of xenobiotic degradation processes benefit from the resulting elimination of potentially harmful compounds, as well as, the addition of potential carbon sources for metabolism. Using the GeoChip 2.0, over 2100 genes involved in xenobiotic degradation were detected. The degradation of BTEX (benzene, toluene, ethylbenzene and xylenes) and related compounds accounted for 42% of the genes identified. An additional 11% were involved in degradation of other aromatics, including chlorinated aromatic, nitoaromatic and heteroaromatic compounds. The next largest group of degradation genes (6.5%) was involved in the degradation of known pesticides, herbicides and fungicides. As a whole, the microbial community associated with *M. faveolata* displayed a wide-range capacity for the degradation of more than 75 xenobiotic compounds.

Discussion

Microbial functional diversity associated with the M. faveolata

Molecular studies from the past 10 years have uncovered a rich microbial community associated with corals (Reviewed in Rosenberg *et al*., 2007). The majority of these studies utilized 16S rDNA methodologies to identify bacterial (Rohwer *et al*., 2001; 2002; Frias-Lopez *et al*., 2002; Bourne and Munn, 2005; Klaus *et al*., 2005; Koren and Rosenberg, 2006; Lampert *et al*., 2008) and archaeal (Kellogg, 2004; Wegley *et al*., 2004) community members. Other studies focused on a particular bacterial or archaeal gene in order to identify potential community members capable of a specific function (Lesser *et al*., 2004; Barneah *et al*., 2007; Beman *et al*., 2007; Siboni *et al*., 2008; Olson *et al*., 2009; Raina *et al*., 2009). More recently, metagenomic techniques were used to identify coral holobiont members and address their potential functional roles as a whole (Yokouchi *et al*., 2006; Wegley *et al*., 2007; Thurber *et al*., 2009). Genomic studies, including the one presented here, identify the presence of specific genes; however, they do not necessarily demonstrate functionality. Nonetheless, several studies indicate that this information is predictive of ecological variation between distinct environments (Dinsdale *et al*., 2008a) and similar environments with varying conditions (Dinsdale *et al*., 2008b). Collectively, these studies have enhanced our understanding of coral-associated microbial communities and highlighted the need to further characterize their role in the coral holobiont. To that end, the present study was the first to investigate a broad (> 10 000) set of biogeochemical cycling genes in the coral holobiont, thereby identifying important metabolic processes potentially carried out by the microbial community.

Interestingly, the relative abundance (i.e. percentage of each gene category) of the five broadest level functional categories examined revealed a consistent pattern across all samples, despite variations in gene number and diversity indices between samples (Fig. 2). This trend persisted even when examining the relative abundance of the 31 more refined functional categories examined. Van Nostrand and colleagues (2009) also noted the same phenomenon in microbial communities from bioreduced uranium-contaminated aquifers characterized using the GeoChip 2.0. Likewise, metagenomic data from the human microbiome also revealed a similarly consistent functional pattern despite high levels of bacterial phyla diversity (Turnbaugh *et al*., 2006). The consistency of functional structure observed in these varied environments suggests that microbial communities in general tend to form a stable functional structure regardless of the individual organisms present.

The large number (6727) and varied origin (archaea, bacteria and fungi) of the biogeochemical cycling genes identified in association with *M. faveolata* provided further support that the coral microbiome is abundant and diverse. It is important to remember that the GeoChip, like all FGAs, are limited to probing for known genes; therefore, our data most likely underestimate the functional genes present. However, the identification of bacterial, archaeal and fungal genes in 31, 24 and 15 of the 31 categories examined, respectively, indicated that all three microbial communities play a much greater role in the coral holobiont than previously known. Moreover, the functional overlap displayed by all three microbial communities suggested a previously unacknowledged

amount of functional redundancy across microbial communities. Future studies attempting to determine the role of these metabolic pathways in the coral holobiont will need to carefully address this issue.

Carbon cycling in the coral holobiont

Historically, carbon cycling in the coral holobiont was characterized with respect to the coral–zooxanthellae relationship (Gattuso *et al.*, 1999). The zooxanthellae were shown to utilize carbon dioxide generated through coral respiration to fuel their own photosynthesis, thereby providing the coral with necessary nutrients (Goreau and Goreau, 1960; Muscatine, 1967; Smith, 1974; Muscatine *et al.*, 1975; Goreau *et al.*, 1979). These interactions established the importance of photosynthetic symbionts as contributors to the overall production of organic carbon in coral ecosystems (Smith, 1973; Barnes, 1987). Since then, studies of coral-associated microorganisms have identified additional photosynthetic symbionts (e.g. cyanobacteria) as part of the coral holobiont, causing speculation that the bacterial community plays a productive role in carbon cycling (Shashar *et al.*, 1994; Frias-Lopez *et al.*, 2003; Lesser *et al.*, 2004; Wegley *et al.*, 2007). In addition, the SML, a complex and variable environment containing polysaccharides, glycoproteins and lipids, provides a carbon-rich substrate for microbial growth (Brown and Bythell, 2005). Our study highlighted the potential for carbon cycling in *M. faveolata* through the identification of microbial genes responsible for carbon fixation and carbon degradation. Both bacterial and archaeal genes necessary for carbon fixation via the Calvin cycle, the reductive acetyl-CoA pathway, and the reverse Kreb's cycle were detected. This indicates that these communities can provide carbon assimilation under variable conditions. All three microbial communities were capable of metabolizing simple sugars (e.g. mannose) as well as more complex carbohydrates, such as cellulose and chitin. An enzyme essential for degradation of the recalcitrant lignin was also detected; however, only fungal species were identified. This is notable when considering the recent observation by Thurber and colleagues (2009) that stressed corals showed an increased association with fungi. It is possible that the coral microbial community's capacity for degradation of specific carbon molecules makes it more suitable for varying environments.

Our study also suggested that *M. faveolata*'s microbiome plays a role in carbon cycling through methane transformations. Methanogenesis is the process by which methanogens, a polyphyletic group of Archaea, form methane during anaerobic respiration (Hallam *et al.*, 2004). Conversely, methanogen-like archaeal groups are capable of oxidizing methane to form carbon dioxide via anaerobic oxidation of methane using similar genes to that involved in methanogenesis (Hallam *et al.*, 2003). Bacteria, known as methanotrophs, are also capable of methane oxidation, albeit via aerobic processing (Hanson and Hanson, 1996). In our study, the presence of *mcr* genes from five groups of *Euryarchaeota* and *mmo/pmo* genes from type I and type II methanotrophs suggested the presence of multiple methane transformation strategies. These data showed that coral-associated bacteria and archaea may potentially play a role in methane transformation through both the consumption of methane flux and as an additional source of fixed carbon compounds.

Nitrogen cycling in the coral holobiont

Previous studies proposed that coral ecosystems are nitrogen-limited (Falkowski *et al.*, 1993) and that inorganic nitrogen limited the growth and abundance of zooxanthellae associated with scleractinian corals (Dubinsky and Jokiel, 1994; Dubinsky and Berman-Frank, 2001). This implies that coral ecosystems have a mechanism to regulate nitrogen levels associated with the coral holobiont. Traditionally, it was thought that the coral host was responsible for regulating nitrogen levels affecting their endosymbionts (Muscatine and D'Elia, 1978; Piniak *et al.*, 2003). However, current evidence strongly suggests that the abundant and diverse prokaryotic communities associated with the coral holobiont also play an important role in nitrogen cycling through multiple processes (Wegley *et al.*, 2007). One of the most discussed possibilities is that of nitrogen fixation. Shashar and colleagues (1994) first detected nitrogen fixation in several coral species via acetylene reduction and subsequently showed the presence of coral-associated bacteria containing the *nifH* gene required for nitrogen fixation in one of those species, *Favia favus*. Similarly, Lesser and colleagues (2004) established that nitrogen-fixing cyanobacteria were associated with *Montastraea cavernosa*, and furthermore that these symbionts provided nitrogen to their coral host via nitrogen fixation (Lesser *et al.*, 2007). Additional nitrogen fixing bacteria have been identified in association with *Porites astreoides* (Wegley *et al.*, 2007) and *Montipora* sp. (Olson *et al.*, 2009). Similar to Olsen and colleagues (2009), we detected a wide range of bacterial *nifH* and *nifD* genes from the classes *Proteobacteria* (subclasses *Alpha* and *Gamma*), *Cyanobacteria*, *Firmicutes* and *Spirochetes*. In addition, archaeal *nifH* and *nifD* genes were identified from three classes of *Euryarchaeota*. These data revealed a much more diverse group of nitrogen-fixing microorganisms than previously known, suggesting a greater potential for nitrogen assimilation by the microbial community.

Nitrification, or the oxidation of ammonia into nitrites and nitrates, is another component of the nitrogen cycle that has been identified in corals (Wafar *et al.*, 1990). This

process was traditionally thought to be performed exclusively by bacteria; however, recent studies have highlighted the probable role of mesophilic crenarchaeota as well (Konneke *et al*., 2005; Prosser and Nicol, 2008). In corals, Beman and colleagues (2007) and Siboni and colleagues (2008) identified a diverse group of coral-associated archaeal *amo* genes, while unable to amplify any bacterial *amo* genes. This suggested that coral-associated archaea could be responsible for coral nitrification. Although the GeoChip does not probe for archaeal nitrification genes, it does contain probes for bacterial *amo* and *hao* genes. We detected over 100 *amo* genes (unidentified bacteria, *Betaproteobacteria* and *Gammaproteobacteria*) in addition to *hao* genes (*Betaproteobacteria*). Our data suggest the coral-associated bacterial community may play a role in coral nitrification, and more comprehensive studies are required in order to discern the relative contributions of these two communities.

Nitrogen can also be cycled between ammonium and organic (or biological) forms via ammonium assimilation and ammonification (Myrold, 1999). Within the coral holobiont, Wegley and colleagues (2007) provided evidence for ammonium assimilation via the fungal community associated with *Porites astreoides*. Likewise, our study identified fungal genes (*gdh*) necessary for glutamate metabolism; moreover, we detected *gdh* genes from archaea and bacteria, implicating all three microbial communities in the recycling of biological nitrogen. In addition, ammonification (e.g. degradation of urea to ammonium) via urease is known to occur in corals (Barnes and Crossland, 1976), and we detected urease genes from all three microbial communities, although the vast majority of these (95%) was identified as *Proteobacteria*.

The final nitrogen cycling process examined was denitrification, the reduction of nitrate to N_2. Our study was the first to detect coral-associated microbial genes specific for denitrification. All four of the denitrification genes (*nar*, *nir*, *nor* and *nos*) investigated were detected in our study. Although the GeoChip only contains bacterial specific probes for the *nar*, *nor* and *nos* genes, the *nir* genes are represented by probes for bacterial, archaeal and fungal genes. We detected *nir* genes from all three communities. This suggested that all three microbial communities examined have the capacity to influence denitrification in the coral holobiont. Interestingly, this meant that collectively the *M. faveolata* microbial community could potentially cycle nitrogen completely from N_2 to ammonium to nitrate and back to N_2, while also contributing to the build-up and break-down of biological nitrogen sources.

Sulfur cycling in the coral holobiont

Although little is known about sulfur cycling in the coral holobiont, bacterial species capable of metabolizing organic sulfur compounds (Wegley *et al*., 2007; Raina *et al*., 2009) have been identified within the coral holobiont. Wegley and colleagues (2007) proposed glutathione as the main source of sulfur for coral-associated microbial communities, while Raina and colleagues (2009) proposed dimethylsulfonopropionate (DMSP) and dimethylsulfide (DMS) as important sources of sulfur in the coral holobiont. Another potential role of sulfate-reducing bacteria is anaerobic methane oxidation as demonstrated in bacterial mats associated with coral-like carbonate structures in the Black Sea (Pimenov and Ivanova, 2005) and in ocean microbial communities (Pernthaler *et al*., 2008). The present study identified 501 bacterial and archaeal *dsr* genes associated with *M. faveolata*, adding inorganic sulfate to the potential sources of sulfur for the coral holobiont. Previously, Barneah and colleagues (2007) identified potential sulfate-reducing bacteria related to the subclass *Deltaproteobacteria* (genus *Desulfovibrio*) in the microbial mat associated with black band disease. Similarly, the present study identified the majority of known *dsr* genes as *Deltaproteobacteria*; however, a variety of genera were represented and *dsr* genes were detected in both healthy and YBD infected colonies of *M. faveolata*.

Variations between healthy and YBD M. faveolata

Our study revealed that the biogeochemical cycling potential of the *M. faveolata*-associated microbial community was significantly different between healthy and YBD colonies. In the SML, we observed significantly increased functional diversity in YBD *M. faveolata* with genes detected from a greater variety of known marine pathogens, including species from the bacterial families *Vibrionaceae* and *Alteromonadaceae* and the fungal genus *Aspergillus*. These findings were consistent with previous reports that coral-associated microbial structure varied between healthy and diseased/stressed corals (Frias-Lopez *et al*., 2002; 2004; Pantos *et al*., 2003; Pantos and Bythell, 2006; Sekar *et al*., 2006; Bourne *et al*., 2007; Sunagawa *et al*., 2009; Thurber *et al*., 2009). The specific changes in community structure were variable depending on the coral species and disease of interest. Similar to our results, Sunagawa and colleagues (2009) reported an increase in bacterial diversity in *M. faveolata* during white plague type II disease using 16S rDNA techniques, with an increase in known coral pathogens such as *Vibrionaceae* and *Alteromonadaceae*. In addition, Thurber and colleagues (2009) reported that the microbial communities of stressed *Porites compressa* colonies tended to exhibit increased numbers of bacteria and fungi associated with marine diseases.

In the *M. faveolata* SML, the greatest functional variation between healthy and YBD SML samples occurred in

cellulose degradation and nitrification. Like many bacteria, the ability of coral-associated microorganisms to utilize specific carbon compounds found in the SML could play an important role either in their survival and fitness or in their regulation of virulence (Poncet *et al*., 2009). Supporting this assumption, Krediet and colleagues (2009) reported that the *Acropora palmata* pathogen *Serratia marcescens* outgrew commensal bacteria when cultured on mucus from *A. palmata* but not on mucus from a non-host coral, *M. faveolata*. Our data show that cellulase gene diversity (number of genes detected) increases drastically between healthy and YBD samples, however, the overall pool of cellulase gene copies (represented by signal intensity) is less dramatically altered. In addition, the overlap of cellulase genes associated with healthy samples to those of YBD samples (81%) reflects the introduction of additional microorganisms to the YBD community rather than a shift from one community to a completely different community. Combined, our data suggest that the introduction of opportunistic or pathogenic organisms better suited towards the metabolism of a specific carbon source plays a role in the YBD process. Notably, one of the cellulase genes detected only in the YBD samples was identified as *Vibrio vulnificus* (YJ016), a known marine pathogen.

Nutrient enrichment, including increased nitrate levels, has been shown to affect coral disease, causing increased virulence of YBD in *Montastraea* sp. (Bruno *et al*., 2003). Our study showed a significant increase in the number of nitrification genes detected in YBD SML samples compared with that of the healthy samples. In addition, our data revealed the presence of all three *amo* subunits necessary for a functional ammonium monooxygenase enzyme only in association with the YBD SML. Although we cannot rule out the possibility that all three subunits may also be present in healthy samples at a lower threshold cutoff (SNR < 2.0), our data suggest an increased potential for nitrification in YBD colonies. We would predict therefore that YBD virulence could also be affected by an increased capacity of the microbial community to transform ammonium into nitrate via nitrification.

Although significant variation between healthy and YBD tissue samples also occurs in cellulose degradation and nitrification, eight additional functional gene categories show significant differences. This suggests a much broader shift of the functional potential associated with *M. faveolata* tissue during YBD, including categories in metal transformation, xenobiotic degradation and nutrient cycling. One possible explanation for this is that the SML, acting as a first line of defence, is initially disrupted by a specific group of organisms better suited for the nutrient profile of *M. faveolata* SML during YBD. The subsequent disruption of the coral holobiont may then allow a more generalized introduction of opportunistic microorganisms into the coral tissue. Alternatively, YBD could cause a general disruption of the coral holobiont as represented in the tissue, which subsequently provides ideal conditions for the introduction of specific opportunistic microorganisms in the altered SML. In either case, an activating cue (e.g. temperature- or density-dependent signalling) would be required for the invasion of pathogenic or opportunistic microorganisms. The identification of potential functional changes between healthy and YBD-associated coral holobionts now allows us to design experiments in a more focused manner in which to address these questions.

Conclusion

Using the GeoChip 2.0, we established that the microbial functional potential associated with *M. faveolata* is abundant and represents genes from diverse groups of organisms. The nutrient cycling capabilities include carbon cycling, nitrogen cycling and sulfate reduction. *Montastraea faveolata* microbial communities also have the potential to regulate metals and to degrade a diverse montage of xenobiotic compounds. The large number of biogeochemical cycling genes identified in this study supports the idea that coral-associated microbial communities contain diverse microorganisms that could fill numerous functional niches. Furthermore, the functional structure of the microbial community associated with healthy and YBD differs significantly. In the SML, these differences appear to be specific to cellulose degradation and nitrification and are distinct from the more generalized changes exhibited by the *M. faveolata* tissue slurry. Therefore, we predict that physiological changes in the coral holobiont allow for colonization of pathogenic and opportunistic microorganisms most suited for efficient carbon and nitrogen cycling. Future studies are needed to elucidate the role of cellulose degradation and nitrification in YBD of *M. faveolata*.

Experimental procedures

Sample collection

All *M. faveolata* SML and tissue slurry samples were collected in March 2007 from the Media Luna reef located ~5 miles south of La Parguera, PR. Triplicate coral samples (SML and tissue) were collected from three *M. faveolata* colonies that appeared visually healthy (designated H1-H3) and from the yellow band of three colonies exhibiting visual signs of YBD (designated D1-D3). The SML samples were collected in 30 ml sterile syringes and coral tissue samples were collected using a stainless steel corer (1 inch) and hammer. Both the SML filled syringes and the tissue cores were placed in individual sterile Whirlpak bags. All samples were kept on ice until reaching the laboratory (~30 min), where they were

immediately transferred to 50 ml Falcon tubes with 20 ml of 5 M guanidinium isothiocyanate (GIT) buffer. Samples were shipped overnight on dry ice to Hollings Marine Laboratory (Charleston, SC, USA), where they were cryopreserved at –20°C.

DNA extractions

Tissue samples were thawed and crushed using a sterile stainless steel pestle, producing a tissue slurry containing mucus, tissue, skeleton and GIT buffer. Thawed *M. faveolata* SML (750 μl) or tissue slurry (750 μl) was incubated with 30 μl of 10% sodium dodecyl sulfate (SDS) for 1 h at 37°C. The samples were then vortexed and n-butanol precipitated. The precipitate was resuspended in 500 μl of 10% cetyltrimethylammonium bromide (CTAB)/5% polyvinyl polypyrrolidone (PVPP) and chloroform extracted. The aqueous phase was re-extracted with an equal volume of phenol/chloroform/isoamyl alcohol (25:24:1), followed by a final chloroform/isoamyl alcohol (24:1) extraction. The aqueous phase was removed and placed in a sterile microcentrifuge tube, and the DNA was ethanol precipitated using 100% ethanol at 2 times the final concentration at –20°C. The DNA pellet was rinsed with 100 μl of 70% ethanol, dried for 30 min at room temperature and resuspended in 100 μl of sterile water. To clean the DNA for amplification, a Wizard Prep purification spin column (Promega A9280, San Luis Obispo, CA, USA) was used per the manufacturer's instructions.

DNA amplification

Community DNA was amplified using whole-community genome amplification with bacteriophage Phi29 DNA polymerase and random priming (TempliPhi Amplification Kit, GE Healthcare, UK) (Wu *et al.*, 2006). Community DNA (0.5 μl of a 1:10 dilution) was denatured at 95°C for 3 min in sample buffer before being amplified in a reaction buffer with Phi29 DNA polymerase at 30°C for 8 h. The reaction was terminated at 65°C for 10 min and stored at 4°C. DNA amplification was confirmed by electrophoresis, in which 2 μl of the amplification reaction was run on a 1% agarose gel containing ethidium bromide.

DNA labelling

For all samples, 20 μl of random primers (8mer) was added to ~3 μg of amplified community DNA and heated at 99.9°C for 5 min. Samples were then immediately chilled on ice. The chilled samples were added to a labelling master mix: 2.5 μl dNTP mix (5 mM dAGC-TP, 2.5 mM dTTP), 1.0 μl Cy5-dUTP (25 nM; Amersham, Piscataway NJ), 80 U Klenow and water to a total of 50 μl. The samples were incubated at 37°C in a thermocycler for 3 h. After the incorporation of Cy5, samples were protected from the light as much as possible. A QIAquick purification kit (Qiagen, Valencia, CA, USA) was used per the manufacturer's instructions to clean labelled DNA, and then the samples were dried in a SpeedVac for 45 min at 45°C (ThermoSavant, Milford, MA, USA).

Functional gene array

Hybridization to the GeoChip 2.0 (He *et al.*, 2007) was performed using a Tecan HS 4800Pro hybridization station (Tecan US) at 35°C plus 50% formamide for 10 h. Technical triplicates were performed for each biological sample ($N = 12$). For all samples, 130 μl of a 40% formamide hybridization mix (52 μl of formamide, 19.5 μl of 20× SSC, 3.9 μl of 10% SDS, 9 μl of 0.1 μg/μl of Herring sperm DNA, 1.1 μl of DTT and 44.4 μl of DI water) was added to the labelled genomic DNA and incubated at 95°C for 5 min and maintained at 60°C until hybridization. Array slides were imaged using a ScanArray Express Microarray Scanner (Perkin Elmer, Waltham, MA, USA) and analysed using ImaGene software 6.0 (Biodiscovery, CA, USA). All hybridized slides underwent quality control determination based on background level, signal level and even hybridization (spatial variation). After normalization, negative spots and poor-quality spots were removed. The signal-to-noise ratio [SNR = (signal mean∗background mean)/(background standard deviation)] was also computed for each spot to discriminate true signals from noise.

Data analysis

All data analysis was performed using the combined results of technical duplicates that provided the closest replication for each biological sample. Technical triplicates were not possible for all 12 samples due to a poor quality determination of two slides. Microarray spots were defined as positive if they were within two standard deviations of the mean (sigma = 2) and had a minimum SNR of 2. For positive qualification of a target gene, at least one-third of the probes were determined to be positive, with a minimum of two positive probes required. Most genes had three probes per array (He *et al.*, 2007). Functional gene diversity assessment, PCA and cluster analysis were performed using the pipeline provided by the Institute for Environmental Genomics at the University of Oklahoma (http://ieg.ou.edu/). For PCA, transformed data (square root of average signal intensity) were used, and cluster analysis was performed using the Bray–Curtis similarity coefficient and pairwise complete-linkage hierarchical clustering. A two-way crossed (with replicates) ANOSIM using 1000 permutations and subsequent SIMPER analysis were performed using the PRIMER program (Clark and Warwick, 2001).

Acknowledgements

This study was supported by a National Science Foundation Biodiversity Surveys and Inventories Grant (DEB0516347) to P.J.M. and a National Science Foundation Graduate Research Fellowship to N.E.K. The work of E.W. was partially supported by the GEF-World Bank Coral Reef Targeted Research and Capacity Building through the Coral Disease Working Group, as well as the NOAA-CRES program (NA170P2919). The GeoChip analysis was supported by the Virtual Institute for Microbial Stress and Survival (http://VIMSS.lbl.gov) supported by the US Department of Energy, Office of Science, Office of Biological and Environmental Research, Genomics Program:GTL through contract DE-AC02-05CH11231 between Lawrence Berkeley National Laboratory and the US Department of Energy. We also thank Dr Erik Sotka at the College of Charleston for helpful discussions regarding data analysis.

References

Amann, R.I., Ludwig, W., and Schleifer, K. (1995) Phylogenetic identification and in situ detection of individual microbial cells without cultivation. *Microbiol Rev* **59:** 143–169.

Badger, M.R., and Bek, E.J. (2008) Multiple rubisco forms in Proteobacteria: their functional significance in relation to CO2 acquisition by the CBB cycle. *J Exp Bot* **59:** 1525–1541.

Baker, A.C. (2003) Flexibility and specificity in coral-algal symbiosis: diversity, ecology, and biogeography of *Symbiodinium*. *Annu Rev Ecol Evol Syst* **34:** 661–689.

Barneah, O., Ben Dov, E., Kramarsky-Winter, E., and Kushmaro, A. (2007) Characterization of black band disease in Red Sea stony corals. *Environ Microbiol* **9:** 1995–2006.

Barnes, R.D. (1987) *Invertebrate Zoology*. Fort Worth, TX, USA: Harcourt Brace Jovanovich College Publishers.

Barnes, D.J., and Crossland, C.J. (1976) Urease activity in the staghorn coral, *Acropora acuminata*. *Comp Biochem Physiol* **55:** 371–376.

Beman, J.M., Roberts, K.J., Wegley, L., Rohwer, F., and Francis, C.A. (2007) Distribution and diversity of archaeal ammonia monooxygenase genes associated with corals. *Appl Environ Microbiol* **73:** 5642–5647.

Bentis, C., Kaufman, L., and Golubic, S. (2000) Endolithic fungi in reef-building corals (order: Scleractinia) are common, cosmopolitan, and potentially pathogenic. *Biol Bull* **198:** 254–260.

Berg, J.M., Tymoczko, J.L., and Stryer, L. (eds) (2002) *Biochemistry*. New York, NY, USA: W.H. Freeman and Company.

Bourne, D., Iida, Y., Uthicke, S., and Smith-Keune, C. (2007) Changes in coral-associated microbial communities during a bleaching event. *ISME J* **2:** 350–363.

Bourne, D.G., and Munn, C.B. (2005) Diversity of bacteria associated with the coral *Pocillopora damicornis* from the Great Barrier Reef. *Environ Microbiol* **7:** 1162–1174.

Brown, B.E., and Bythell, J.C. (2005) Perspectives on mucus secretion in reef corals. *Mar Ecol Prog Ser* **296:** 291–309.

Bruckner, A.W., and Bruckner, R.J. (2006) Consequences of yellow band disease (CYBD) on *Montastraea annularis* (species complex) populations on remote reefs off Mona Island, Puerto Rico. *Dis Aquat Organ* **69:** 67–73.

Bruno, J.F., Petes, L.E., Harvell, C.D., and Hettinger, A. (2003) Nutrient enrichment can increase the severity of coral diseases. *Ecol Lett* **6:** 1056–1061.

Buchanan, B.B., and Arnon, D.I. (1990) A reverse krebs cycle in photosynthesis: consensus at last. *Photosynth Res* **24:** 47–53.

Casas, V., Kline, D.I., and Wegley, L., YuY., Breitbart, M., and Rohwer, F. (2004) Widespread association of a Rickettsiales-like bacterium with reef-building corals. *Environ Microbiol* **6:** 1137–1148.

Cervino, J., Goreau, T.J., Nagelkerken, I., Smith, G., and Hayes, R. (2001) Yellow band and dark spot syndromes in Caribbean corals: distribution rate of spread cytology and effects on abundance and division rate of zooxanthellae. *Hydrobiologia* **460:** 53–63.

Cervino, J.M., Hayes, R., Goreau, T.J., and Smith, G.W. (2004) Zooxanthellae regulation in yellow blotch/band and other coral diseases contrasted with temperature related bleaching: in situ destruction vs. expulsion. *Symbiosis* **37:** 63–85.

Clark, K.R., and Warwick, R.M. (2001) *Change in Marine Communities: An Approach to Statistical Analysis and Interpretation*, 2nd edn. Plymouth, UK: PRIMER-E.

Coral Disease Working Group (2007) Breaking waves: coral disease, environmental drivers, and the balance between coral and microbial associates. *Oceanography* **20:** 58–81.

Croquer, A., and Weil, E. (2009) Spatial variability in distribution and prevalence of Caribbean scleractinian coral and octocoral diseases. Ii. Genera-level analysis. *Dis Aquat Organ* **83:** 209–222.

Dinsdale, E.A., Edwards, R.A., Hall, D., Angly, F., Breitbart, M., Brulc, J.M., *et al.* (2008a) Functional metagenomic profiling of nine biomes. *Nature* **452:** 629–632.

Dinsdale, E.A., Pantos, O., Smriga, S., Edwards, R.A., Angly, F., Wegley, L., *et al.* (2008b) Microbial ecology of four coral atolls in the Northern Line Islands. *PLoS ONE* **3:** e1584.

Dubinsky, Z., and Berman-Frank, I. (2001) Uncoupling primary production from population growth in photosynthesizing organisms in aquatic ecosystems. *Aquat Sci* **63:** 4–17.

Dubinsky, Z., and Jokiel, P.L. (1994) Ratio of energy and nutrient fluxes regulates symbiosis between zooxanthellae and corals. *Pacific Sci* **48:** 313–324.

Falkowski, P.G., Dubinsky, Z., Muscatine, L., and McCloskey, L. (1993) Population control in symbiotic corals: ammonium ions and organic materials maintain the density of zooxanthellae. *Bioscience* **43:** 606–611.

Ferrier-Pages, C., Gattuso, J.P., Cauwet, G., Jaubert, J., and Allemand, D. (1998) Release of dissolved organic carbon and nitrogen by the zooxanthellate coral *Galaxea fascicularis*. *Mar Ecol Prog Ser* **172:** 265–274.

Frias-Lopez, J., Zerkle, A.L., Bonheyo, G.T., and Fouke, B.W. (2002) Partitioning of bacterial communities between seawater and healthy, black band diseased, and dead coral surfaces. *Appl Environ Microbiol* **68:** 2214–2228.

Frias-Lopez, J., Bonheyo, G.T., Jin, Q.S., and Fouke, B.W. (2003) *Cyanobacteria* associated with coral black band disease in Caribbean and Indo-pacific reefs. *Appl Environ Microbiol* **69:** 2409–2413.

Frias-Lopez, J., Klaus, J.S., Bonheyo, G.T., and Fouke, B.W. (2004) Bacterial community associated with black band disease in corals. *Appl Environ Microbiol* **70:** 5955–5962.

Fuhrman, J.A., and Campbell, L. (1998) Microbial microdiversity. *Nature* **393:** 410–411.

Gattuso, J.P., Allemand, D., and Frankignoulle, M. (1999) Photosynthesis and calcification at cellular, organismal and community levels in coral reefs: a review on interactions and control by carbonate chemistry. *Am Zool* **39:** 160–183.

Gentry, T.J., Wickham, G.S., Schadt, C.W., He, Z., and Zhou, J. (2006) Microarray applications in microbial ecology research. *Microb Ecol* **52:** 159–175.

Goreau, T.F., and Goreau, N.I. (1960) Distribution of labeled carbon in reef-building corals with and without zooxanthellae. *Science* **131:** 668–669.

Goreau, T.F., Goreau, N.I., and Goreau, T.J. (1979) Corals and coral reefs. *Sci Am* **241:** 124–136.

Hallam, S.J., Girguis, P.R., Preston, C.M., Richardson, P.M., and DeLong, E.F. (2003) Identification of methyl coenzyme

M reductase A (*mcrA*) genes associated with methane-oxidizing archaea. *Appl Environ Microbiol* **69:** 5483–5491.
Hallam, S.J., Putnam, N., Preston, C.M., Detter, J.C., Rokhsar, D., Richardson, P.M., and DeLong, E.F. (2004) Reverse methanogenesis: testing the hypothesis with environmental genomics. *Science* **305:** 1457–1461.
Hanson, R.S., and Hanson, T.E. (1996) Methanotrophic bacteria. *Microbiol Rev* **60:** 439–471.
Harvell, C.D., Jordan-Dahlgren, E., Merkel, S., Rosenberg, E., Raymundo, L., Smith, G., *et al.* (2007) Coral disease, environmental drivers and the balance between coral and microbial associates. *Oceanography* **20:** 58–81.
Harvell, C.D., Altizer, S., Cattadori, I.M., Harrington, L., and Weil, E. (2009) Climate change and wildlife diseases: when does the host matter the most? *Ecology* **90:** 912–920.
He, Z., Gentry, T.J., Schadt, C.W., Wu, L., Liebich, J., Chong, S.C., *et al.* (2007) Geochip: a comprehensive microarray for investigating biogeochemical, ecological and environmental processes. *Int Soc Microb Ecol J* **1:** 67–77.
Jetten, M.S.M. (2008) The microbial nitrogen cycle. *Environ Microbiol* **10:** 2903–2909.
Kellogg, C.A. (2004) Tropical archaea: diversity associated with the surface microlayer of corals. *Mar Ecol Prog Ser* **273:** 81–88.
Klaus, J.S., Frias-Lopez, J., Bonheyo, G.T., Heikoop, J.M., and Fouke, B.W. (2005) Bacterial communities inhabiting the healthy tissues of two Caribbean reef corals: Interspecific and spatial variation. *Coral Reefs* **24:** 129–137.
Knowlton, N., and Rohwer, F. (2003) Multispecies microbial mutualisms on coral reefs: the host as habitat. *Am Nat* **162:** S51–S62.
Konneke, M., Bernhard, A.E., de la Torre, J.R., Walker, C.B., Waterbury, J.B., and Stahl, D.A. (2005) Isolation of an autotrophic ammonia-oxidizing marine archaeon. *Nature* **437:** 543–546.
Koren, O., and Rosenberg, E. (2006) Bacteria associated with mucus and tissues of the coral *Oculina patagonica* in summer and winter. *Appl Environ Microbiol* **72:** 5254–5259.
Krediet, C.J., Ritchie, K.B., Cohen, M., Lipp, E.K., Sutherland, K.P., and Teplitski, M. (2009) Utilization of mucus from the coral *Acropora palmata* by the pathogen *Serratia marcescens* and by environmental and coral commensal bacteria. *Appl Environ Microbiol* **75:** 3851–3858.
Lampert, Y., Kelman, D., Nitzan, Y., Dubinsky, Z., Behar, A., and Hill, R.T. (2008) Phylogenetic diversity of bacteria associated with the mucus of Red Sea corals. *FEMS Microbiol Ecol* **64:** 187–198.
Leggat, W., Ainsworth, T., Bythell, J.C., Dove, S., Gates, R.D., Hoegh-Guldberg, O., *et al.* (2007) The hologenome theory disregards the coral holobiont. *Nat Rev Microbiol* **5:** doi: 10.1038/nrmicro1635_c1.
Lesser, M.P., Mazel, C.H., Gorbunov, M.Y., and Falkowski, P.G. (2004) Discovery of symbiotic nitrogen-fixing cyanobacteria in corals. *Science* **305:** 997–1000.
Lesser, M.P., Falcon, L.I., Rodriguez-Roman, A., Enriquez, S., Hoegh-Guldberg, O., and Iglesias-Prieto, R. (2007) Nitrogen fixation by symbiotic cyanobacteria provides a source of nitrogen for the scleractinian coral *Montastraea cavernosa*. *Mar Ecol Prog Ser* **347:** 143–152.
Liang, Y., Wang, J., Van Nostrand, J.D., Zhou, J., Zhang, X., and Li, G. (2009) Microarray-based functional gene analysis of soil microbial communities in ozonation and biodegradation of crude oil. *Chemosphere* **75:** 193–199.
Lloyd, J.R. (2005) Dissimilatory metal transformations by microorganisms. In *Encyclopedia of Life Sciences*. Chichester, England: John Wiley & Sons, doi: 10.1038/npg.els.0000474.
Mason, O.U., Di Meo-Savoie, C.A., Van Nostrand, J.D., Zhou, J., Fisk, M.R., and Giovannoni, S.J. (2009) Prokaryotic diversity, distribution, and insights into their role in biogeochemical cycling in marine basalts. *ISME J* **3:** 231–242.
Muller-Parker, G., and D'Elia, C.F. (1997) *Interactions Between Corals and Their Symbiotic Algae*. New York, NY, USA: Chapman & Hall.
Muscatine, L. (1967) Glycerol excretion by symbiotic algae from corals and tridacna and its control by the host. *Science* **156:** 516–519.
Muscatine, L. (1973) Nutrition of corals. In *Biology and Geology of Coral Reefs*. Jones, O.A., and Endean, R. (eds). New York, NY, USA: Academic Press, pp. 77–115.
Muscatine, L. (1980) *Productivity of Zooxanthellae*. New York, NY, USA: Plenum.
Muscatine, L. (1990) The role of symbiotic algae in carbon and energy flux in reef corals. In *Ecosystems of the World: 25. Coral Reefs*. Dubinsky, Z. (ed.). New York, NY, USA: Elsevier Scientific Publishing, pp. 75–88.
Muscatine, L., and D'Elia, C.F. (1978) The uptake, retention, and release of ammonium by reef corals. *Limnol Oceanogr* **23:** 725–734.
Muscatine, L., Pool, R.R., and Trench, R.K. (1975) Symbiosis of algae and invertebrates: aspects of the symbiont surface and the host–symbiont interface. *Trans Am Microsc Soc* **94:** 450–469.
Muscatine, L., Falkowski, P.G., Porter, J.W., and Dubinsky, Z. (1984) Fate of photosynthetic fixed carbon in light- and shade-adapted colonies of the symbiotic coral *Stylophora pistillata*. *Proc R Soc Lond B* **222:** 181–202.
Myrold, D.D. (1999) Transformations of nitrogen. In *Principals and Applications of Soil Microbiology*. Sylvia, D.M., Fuhrmann, J.J., Hartel, P.G., and Zuberer, D.A. (eds). Upper Saddle River, NJ, USA: Prentice Hall.
Olson, N.D., Ainsworth, T.D., Gates, R.D., and Takabayashi, M. (2009) Diazotrophic bacteria associated with Hawaiian *Montipora* corals: diversity and abundance in correlation with symbiotic dinoflagellates. *J Exp Mar Biol Ecol* **371:** 140–146.
Pantos, O., and Bythell, J.C. (2006) Bacterial community structure associated with white band disease in the elkhorn coral *Acropora palmata* determined using culture-independent 16s rRNA techniques. *Dis Aquat Organ* **69:** 79–88.
Pantos, O., Cooney, R.P., Le Tissier, M.D., Barer, M.R., O'Donnell, A.G., and Bythell, J.C. (2003) The bacterial ecology of a plague-like disease affecting the Caribbean coral *Montastrea annularis*. *Environ Microbiol* **5:** 370–382.
Pernthaler, A., Dekas, A.E., Brown, C.T., Goffredi, S.K., Embaye, T., and Orphan, V.J. (2008) Diverse syntrophic partnerships from deep-sea methane vents revealed by direct cell capture and metagenomics. *Proc Natl Acad Sci USA* **105:** 7052–7057.
Pimenov, N.V., and Ivanova, A.E. (2005) Anaerobic methane oxidation and sulfate reduction in bacterial mats on coral-

like carbonate structures in the Black Sea. *Microbiology* **74:** 362–370.
Piniak, G.A., Lipschultz, F., and McClelland, J. (2003) Assimilation and partitioning of prey nitrogen within two anthozoans and their endosymbiotic zooxanthellae. *Mar Ecol Prog Ser* **262:** 125–136.
Poncet, S., Milohanic, E., Maze, A., Abdallah, J.N., Ake, F., Larribe, M., *et al.* (2009) Correlations between carbon metabolism and virulence in bacteria. *Contrib Microbiol* **16:** 88–102.
Prosser, J.I., and Nicol, G.W. (2008) Relative contributions of archaea and bacteria to aerobic ammonia oxidation in the environment. *Environ Microbiol* **10:** 2931–2941.
Ragsdale, S.W. (1991) Enzymology of the acetyl-CoA pathway of CO_2 fixation. *Crit Rev Biochem Mol Biol* **26:** 3–4.
Raina, J., Tapiolas, D.M., Willis, B., and Bourne, D. (2009) Coral-associated bacteria and their role in the biogeochemical cycling of sulfur. *Appl Environ Microbiol* **75:** 3492–3501.
Richardson, L. (2004) Black band disease. In *Coral Health and Disease*. Rosenberg, E., and Loya, Y. (eds). Berlin, Germany: Springer, pp. 325–336.
Rodriguez-Martinez, E.M., Perez, E.X., Schadt, C.W., Zhou, J., and Massol-Deya, A.A. (2006) Microbial diversity and bioremediation of a hydrocarbon-contaminated aquifer (Vega Baja, PuertoRico). *Int J Environ Res Public Health* **3:** 292–300.
Rohwer, F., Breitbart, M., Jara, J., Azam, F., and Knowlton, N. (2001) Diversity of bacteria associated with the Caribbean coral *Montastraea franksi*. *Coral Reefs* **20:** 85–91.
Rohwer, F., Seguritan, V., Azam, F., and Knowlton, N. (2002) Diversity and distribution of coral-associated bacteria. *Mar Ecol Prog Ser* **243:** 1–10.
Rosenberg, E., and Loya, Y. (2004) *Coral Health and Disease*. New York, NY, USA: Springer-Verlag.
Rosenberg, E., Koren, O., Reshef, L., Efrony, R., and Zilber-Rosenberg, I. (2007) The role of microorganisms in coral health, disease and evolution. *Nature* **5:** 355–362.
Sekar, R., Mills, D.K., Remily, E.R., Voss, J.D., and Richardson, L.L. (2006) Microbial communities in the surface mucopolysaccharide layer and the black band microbial mat of black band-diseased *Siderastrea siderea*. *Appl Environ Microbiol* **72:** 5963–5973.
Shashar, N., Cohen, Y., Loya, Y., and Sar, N. (1994) Nitrogen fixation (acetylene reduction) in stony corals: evidence for coral bacteria interactions. *Mar Ecol Prog Ser* **11:** 259–264.
Siboni, N., Ben Dov, E., Sivan, A., and Kushmaro, A. (2008) Global distribution and diversity of coral-associated archaea and their possible role in the coral holobiont nitrogen cycle. *Environ Microbiol* **10:** 2979–2990.
Silver, S., and Phung, L.T. (2005) A bacterial view of the periodic table: genes and proteins for toxic inorganic ions. *J Ind Microbiol Biotechnol* **32:** 587–605.
Smith, S.V. (1973) Carbon dioxide dynamics: a record of organic carbon production, respiration, and calcification in the Eniwetok reef flat community. *Limnol Oceanogr* **18:** 106–120.
Smith, D.C. (1974) Transport from symbiotic algae and symbiotic chloroplasts to host cells. *Symp Soc Exp Biol* **28:** 485–520.
Stat, M., Morris, E., and Gates, R.D. (2008) Functional diversity in coral-dinoflagellate symbiosis. *Proc Natl Acad Sci USA* **105:** 9256–9262.
Sunagawa, S., DeSantis, T.Z., Piceno, Y., Brodie, E., DeSalvo, M.K., Voolstra, C.R., *et al.* (2009) Bacterial diversity and white plague disease-associated community changes in the Caribbean coral *Montastraea faveolata*. *ISME J* **3:** 1–10.
Szmant, A.M., Ferrer, L.M., and FitzGerald, L.M. (1990) Nitrogen excretion and O : N ratios in reef corals: evidence for conservation of nitrogen. *Mar Biol* **104:** 119–127.
Thornhill, D.J., LaJeunesse, T.C., Kemp, D.W., Fitt, W.K., and Schmidt, G.W. (2006) Multi-year, seasonal genotypic surveys of coral-algal symbiosis reveal prevalent stability or post-bleaching reversion. *Mar Biol* **148:** 711–722.
Thurber, R.V., Willner-Hall, D., Rodriguez-Mueller, B., Desnues, C., Edwards, R.A., Angly, F., *et al.* (2009) Metagenomic analysis of stressed coral holobionts. *Environ Microbiol* **11:** 2148–2163.
Turnbaugh, P.J., Ley, R.E., Mahowald, M.A., Magrini, V., Mardis, E.R., and Gordon, J.I. (2006) An obesity-associated gut microbiome with increased capacity for energy harvest. *Nature* **444:** 1027–1031.
Van Nostrand, J.D., Wu, W., Wu, L., Deng, Y., Carley, J., Carroll, S., *et al.* (2009) Geochip-based analysis of functional microbial communities during the reoxidation of a bioreduced uranium-contaminated aquifer. *Environ Sci Technol* **11:** 2611–2626.
Wafar, M., Wafar, S., and David, J.J. (1990) Nitrification in reef corals. *Limnol Oceanogr* **35:** 725–730.
Waldron, P.J., Wu, L., Van Nostrand, J.D., Schadt, C.W., He, Z., Watson, D.B., *et al.* (2009) Functional gene array-based analysis of microbial community structure in groundwaters with a gradient of contaminant levels. *Environ Sci Technol* **43:** 3529–3534.
Wang, F., Zhou, H., Meng, J., Peng, X., Jiang, L., Sun, P., *et al.* (2009) Geochip-based analysis of metabolic diversity of microbial communities at the Juan de Fuca Ridge hydrothermal vent. *Proc Natl Acad Sci USA* **106:** 4840–4845.
Wegley, L., Yu, Y., Breitbart, M., Casas, V., Kline, D.I., and Rohwer, F. (2004) Coral-associated archaea. *Mar Ecol Prog Ser* **273:** 89–96.
Wegley, L., Edwards, R.A., Rodriguez-Brito, B., Hong, L., and Rohwer, F. (2007) Metagenomic analysis of the microbial community associated with the coral *Porites asteroides*. *Environ Microbiol* **9:** 2707–2719.
Weil, E., Smith, G., and Gil-Agudelo, D.L. (2006) Status and progress in coral reef disease research. *Dis Aquat Organ* **69:** 1–7.
Wu, L., Kellogg, L., Devol, A.H., Tiedje, J., and Zhou, J. (2008) Microarray-based characterization of microbial community functional structure and heterogeneity in marine sediments from the Gulf of Mexico. *Appl Environ Microbiol* **74:** 4516–4529.
Wu, L., Liu, X., Schadt, C.W., and Zhou, J. (2006) Micro-array based analysis of subnanogram quantities of microbial community DNAs by using whole-community genome amplification. *Appl Environ Microbiol* **72:** 4931–4941.
Wu, L., Thompson, D.K., Li, G., Hurt, R.A., Tiedje, J., and Zhou, J. (2001) Development and evaluation of functional gene arrays for detection of selected genes in the environment. *Appl Environ Microbiol* **67:** 5780–5790.

Yergeau, E., Schoondermark-Stolk, S.A., Brodie, E., Dejean, S., DeSantis, T.Z., Gonçalves, O., *et al.* (2008) Environmental microarray analyses of Antarctic soil microbial communities. *ISME J* **3:** 340–351.

Yokouchi, H., Fukuoka, Y., Mukoyama, D., Calugay, R., Takeyama, H., and Matsunaga, T. (2006) Whole-metagenome amplification of a microbial community associated with scleractinian coral by multiple displacement amplification using Phi 29 polymerase. *Environ Microbiol* **8:** 1155–1163.

Yonge, C.M. (1929) Progress of the Great Barrier Reef expedition. *Nature* **123:** 89–99.

Yonge, C.M. (1931) The significance of the relationship between corals and zooxanthellae. *Nature* **128:** 309–311.

Zehr, J.P., Jenkins, B.D., Short, S.M., and Steward, G.F. (2003) Nitrogenase gene diversity and microbial community structure: a cross-system comparison. *Environ Microbiol* **5:** 539–554.